

11. DATA REPORT: CARBONATE AND BARITE TRENDS ACROSS THE EOCENE/OLIGOCENE BOUNDARY AT SHATSKY RISE, ODP LEG 198¹

Kristen B. Averyt,² Michael Calhoun,² Lyndsie Schmalz,² and
Adina Paytan²

ABSTRACT

The barite and CaCO₃ content (in weight percent) of marine sediments can be used to determine spatial and temporal changes in export production (organic and carbonate carbon flux) and/or CaCO₃ preservation (inorganic carbon burial). Here we report barite and CaCO₃ content in Eocene/Oligocene (E/O) boundary sediments from locations drilled on Shatsky Rise during Ocean Drilling Program Leg 198. Records of these indexes may be used along with other data to determine how the major E/O boundary climatic transition (initiation of Antarctic glaciation and resultant ocean–climate system changes) affected marine export production/preservation at Shatsky Rise. Such data are necessary to elucidate the timing and phasing of changes in the carbon cycle relative to fluctuations in oceanographic conditions across this climatically important interval.

INTRODUCTION

Reconstructions of oceanographic physical and chemical properties through the Eocene–Oligocene transition are based on data sets derived predominantly from the Atlantic and Indian Oceans (e.g., Miller et al., 1987; Zachos et al., 1996). The sedimentary sections recovered from Shatsky Rise (northwest Pacific Ocean) during Ocean Drilling Program

¹Averyt, K.B., Calhoun, M., Schmalz, L., and Paytan, A., 2005. Data report: Carbonate and barite trends across the Eocene/Oligocene boundary at Shatsky Rise, ODP Leg 198. *In* Bralower, T.J., Premoli Silva, I., and Malone, M.J. (Eds.), *Proc. ODP, Sci. Results*, 198, 1–16 [Online]. Available from World Wide Web: <http://www-odp.tamu.edu/publications/198_SR/VOLUME/CHAPTERS/106.PDF>. [Cited YYYY-MM-DD]
²Stanford University, Department of Geological and Environmental Science, 320 Braun Hall, Stanford CA 94305, USA. Correspondence author: kaveryt@pangea.stanford.edu

(ODP) Leg 198 provide an opportunity to expand the available paleo-oceanographic record to include how the Pacific Ocean responded to the abrupt climate changes across the Eocene/Oligocene (E/O) boundary (Shipboard Scientific Party, 2002). These data will complement other records derived from ODP Leg 199 equatorial Pacific Ocean sediments. Records generated from marine barite and carbonate content and accumulation rates of the Eocene–Oligocene sedimentary sections at Sites 1209–1211 should provide insight into how export production varied relative to the onset of global “icehouse” conditions, thus contributing to a more robust understanding of how global ocean chemistry (e.g., carbonate compensation depth [CCD]) and circulation, the carbon cycle, and climate developed through this key transition.

The Eocene/Oligocene Boundary

The Eocene–Oligocene transition is characterized by a gradual decrease in global temperatures and the ultimate onset of Antarctic glaciation (Lear et al., 2000; Zachos et al., 1996, 2001). The transition to Oligocene icehouse conditions occurred over millions of years with most of the cooling occurring prior to the Oi-1 event (33.15–33.5 Ma), where Mg/Ca and oxygen isotope data indicate deep-sea water cooled by ~2°C and large permanent ice sheets formed on the Antarctic continent (DeConto and Pollard, 2003; Lear et al., 2000; Miller et al., 1991; Wright and Miller, 1993; Zachos et al., 1994, 1996, 2001). Several tectonic (geo-oceanographic) events and changes in oceanographic biogeochemical processes occurred during this time interval and may be related to the global cooling and formation of Antarctic ice sheets. These processes include

- The separation of Australia and South America from Antarctica (between 32 and 38 Ma), which formed the Tasman Sea and ultimately the Southern Ocean and, as a consequence, thermally isolated the Antarctic continent (Exon et al., 2002; Kennett, 1977; Kennett and Shackleton, 1976);
- Increased chemical weathering as suggested from seawater Sr and Os isotope records, related to a fall in sea level and possibly also Tibetan Plateau uplift (Ravizza and Peucker-Ehrenbrink, 2003; Raymo and Ruddiman, 1992);
- Enhanced terrestrial carbon drawdown due to the expansion of grasslands (Retallack, 2001); and
- Increased organic carbon burial in the deep sea (Diester-Haass and Zahn, 1996; Nilsen et al., 2003), possibly caused by an increase in ocean productivity (Diester-Haass, 1995; Diester-Haass and Zahn, 1996; Ehrmann and Mackensen, 1992).

Many of these processes are directly related to the global carbon cycle, either as cause or effect, and have the potential to influence atmospheric CO₂ concentrations.

Long-term CO₂ proxy records indicate a steady drawdown of atmospheric CO₂ through the Cenozoic (Pagani et al., 1999; Pearson and Palmer, 2000; Retallack, 2001). DeConto and Pollard (2003) used a global circulation model to show that continuous depletion of pCO₂, amplified by Milankovitch forcing and ice-albedo feedbacks, could cause significant temperature reduction resulting in formation of permanent continental ice sheets in high latitudes. It is clear from the relationship between global cooling and pCO₂ that it is important to constrain the

processes influencing the carbon cycle (and thus atmospheric CO₂), as well as any resultant outcomes of such perturbations, through the E/O boundary.

One of the major response/forcing mechanisms in the global carbon cycle is oceanic export productivity: the process by which biologically sequestered carbon is transferred to the deep ocean. Typically, although not always (e.g., Goni et al., 1998), high export production corresponds with high organic matter burial in marine sediments (Müller and Suess, 1979; Sarnthein et al., 1988). The supply of organic carbon to pelagic sediments relative to inorganic carbon, and its burial efficiency, affect the partitioning of CO₂ between the oceanic and atmospheric reservoirs. As a result, fluctuations in organic carbon export and burial can influence pCO₂. High-resolution $\delta^{13}\text{C}$ data analyses of benthic foraminifers and bulk calcite show a positive excursion through the E/O boundary that is recognized globally (Zachos et al., 2001), indicating a change in partitioning of carbon among different reservoirs (i.e., lithosphere, ocean, and atmosphere) and an increase in the ratio of organic carbon to carbonate storage (e.g., Diester-Haass and Zahn, 1996). To define the role of changes in export production as either a causal or feedback response mechanism in regulating climate and to evaluate the relationship between productivity and climate, it is important to quantify changes in organic carbon flux (export productivity) and carbonate carbon burial across the E/O boundary.

Productivity changes associated with the E/O boundary have been documented in both terrestrial and deep-sea sediment sequences using proxies that include accumulation and preservation of diatoms, isotopic records derived from bulk calcite and foraminifers, and bulk sedimentary geochemical analyses (Diester-Haass, 1995, 1996; Diester-Haass and Zahn, 1996; Ehrmann and Mackensen, 1992). In general, such records show an increase in diatom productivity, which may have increased the organic carbon to calcite burial ratio, thus contributing to the global $\delta^{13}\text{C}$ excursion (Zachos et al., 2001). Although the $\delta^{13}\text{C}$ excursion has been recorded in sediments from all ocean basins, there are no productivity proxy records across the E/O boundary available from the tropical or subtropical Pacific. The reason for this paucity of data is that few sections have been drilled from the Pacific that contain complete Eocene–Oligocene transitions. This has been rectified recently by the drilling activities of ODP Legs 198 and 199.

Paleoproductivity Proxies

Significant work has focused on developing proxies for past productivity and interpreting these indexes in terms of organic carbon export. These include direct measurements of organic carbon accumulation in sediments, biogenic opal accumulation, calcium carbonate accumulation, foraminiferal assemblage data, and $\delta^{13}\text{C}$ fluctuations (e.g., Broecker and Peng, 1982; Müller and Suess, 1979; Sarnthein et al., 1988; Tappan, 1968; Calvert, 1966; Herguera, 2000; Berger et al., 1989; Herguera and Berger, 1991; Loubere, 1999). However, the multiple processes that influence these properties, including changes in ocean circulation, dissolution, diagenesis, and nutrient availability, complicate interpretations of these proxies. For example, although the carbonate flux in sediment traps show a good correlation with organic carbon flux under certain conditions in the open ocean above the lysocline (Deuser et al., 1981; Ruhlemann et al., 1996), interpretations of down-core variations in carbonate accumulation are complicated by dissolu-

tion caused by a temporally variant position of the lysocline and CCD. Carbonate dissolution depends on water chemistry, circulation, water temperature and depth, organic matter content in the sediment, changes in the relative quantities of various calcareous shells with different dissolution susceptibility, and other factors. Consequently, it is necessary to integrate several different proxies in order to differentiate productivity signals from the other primary and secondary processes.

One of the most widely used paleoproductivity proxies is excess Ba accumulation in sediments (defined as the Ba not associated with terrigenous matter) (as in Bains et al., 2000; Bonn et al., 1998; Dymond et al., 1992; Faul et al., 2003; Francois et al., 1995; Klump et al., 2001; Nilsen et al., 2003; Nurnberg et al., 1997; Pfeifer et al., 2001). This application is based on the strong relationship between excess Ba and organic carbon fluxes observed in sediment traps (Dymond et al., 1992; Francois et al., 1995) and the high excess Ba or barite accumulation rate in sediment underlying areas of high productivity (Eagle et al., 2003; Gingele and Dahmke, 1994; Goldberg et al., 1969; Paytan et al., 1996; Revelle, 1955). Because marine barite (BaSO_4) is the particulate form of Ba related to export production (Bishop, 1988; Dymond et al., 1992; Paytan et al., 1996; Eagle et al., 2003), determining barite accumulation rates in pelagic sediments is a more direct indicator of export productivity. Barite precipitates in the water column in microenvironments within decaying organic matter and other biogenic debris. The microenvironments become supersaturated with respect to barite because Ba is released from decaying organic matter (Bishop, 1988; Dehairs et al., 1992; Ganeshram et al., 2003). Because the accumulation of marine barite is directly proportional to export production in the overlying water column (Eagle et al., 2003; Paytan et al., 1996), the barite accumulation rate in marine sediments is a good indicator of past changes in export production (Paytan et al., 1996; Eagle et al., 2003). Although the water column is, in general, undersaturated with respect to barite, sediment pore waters in many cases remain saturated, resulting in ~30% preservation of the barite flux that is deposited in marine sediments underlying areas of high biological productivity (McManus et al., 2002; Paytan and Kastner, 1996). After burial, marine barite is preserved in sediments where pore water sulfate is not significantly depleted because the sulfate reduction reaction will proceed to “dissolve” particulate barite once pore water sulfate has been consumed (Paytan and Kastner, 1996).

Comparison of marine barite accumulation trends with those of carbonate content should provide insight into variations in export production and carbonate preservation prior to and after the onset of icehouse conditions and may reveal changes in organic matter flux to the sediment (i.e., export production). During Leg 198, complete E/O boundary sections were acquired in multiple holes from Sites 1208–1211 in the Pacific Ocean (Shipboard Scientific Party, 2002). The sedimentary sections from Shatsky Rise expand the global data set to include the tropical/subtropical Pacific Ocean and have the potential to contribute to a better understanding about how changes in ocean productivity drove or responded to changes in pCO_2 .

METHODS

Sampling of Sedimentary Sections

Complete E/O boundary sections were recovered at Sites 1208–1211 (Shipboard Scientific Party, 2002). The transition from the Eocene to Oligocene was identified by an observed change in sediment color and composition from light brown to white nannofossil ooze, which was recorded in the in color reflectance data (Shipboard Scientific Party, 2002). This change is interpreted as a deepening of the CCD, which is also observed in other deep-sea sedimentary records (see Zachos et al., 2001). At Site 1208, the interval was condensed and could not be sampled at a high enough resolution to yield meaningful data (Shipboard Scientific Party, 2002). The exact location of the E/O boundary and age models will be determined based on $\delta^{18}\text{O}$ analyses of benthic foraminifers to be collected by other shipboard scientists.

Using the lithologic change in the sediment sections and the color reflectance records as guidelines, sediment samples (40 cm^3) were collected at $\sim 20\text{-cm}$ intervals across the E/O boundaries in Holes 1209A, 1209B, 1209C, 1210A, 1210B, 1211A, 1211B, and 1211C. Each 40-cm^3 sediment sample was split into three parts: the coarse fraction ($>63\ \mu\text{m}$) was separated from 20 cm^3 of the original sample; 2 cm^3 was used for carbonate analyses; and the remaining 18 cm^3 was combined with the fine fractions from the 20-cm^3 aliquot and used for barite separations.

Barite Separation Procedure

The pore water sulfate concentrations through the E/O boundaries recovered on Shatsky Rise do not fall below 19 mM (Shipboard Scientific Party, 2002). Assuming that the pore waters have retained such sulfate content through time at Sites 1209–1211 and that the mechanisms governing barite formation and preservation have remained constant, the weight percent barite data reported here should not be affected by changes in barite preservation and should be proportional to carbon export.

Barite was separated from marine sediment using a sequential leaching procedure that included reaction with hydrochloric acid, warm (50°C) sodium hypochlorite (5%), hydroxylamine in acetic acid, and an HF- HNO_3 mixture (Eagle et al., 2003; Paytan et al., 1996). This procedure eliminates carbonates, oxidizes organic matter, removes transition metal oxyhydroxides, dissolves siliceous material, and removes fluorides. The yield of this separation has been determined to be $>90\%$, and the reproducibility of weight percent analyses is $\sim 10\%$ (Eagle et al., 2003). Scanning electron microscope (SEM) screening of select barite separates recovered from the sampled sediments indicates that residues are $>80\%$ barite.

Carbonate Analysis Procedure

For carbonate analyses, $\sim 2\text{ cm}^3$ of bulk sediment was dried at 50°C and ground to a uniform powder. The CaCO_3 content was determined using a Coulometrics UIC coulometer. The weight percent CaCO_3 calculation below assumes that all carbon was derived from calcite.

$$\text{CaCO}_3\ (\text{wt}\%) = (\text{count carbon} - \text{blank})/\text{total weight}/0.12011.$$

Blank samples typically yielded values of 1–2 μg carbon, which was subtracted from the measured sample carbon. The instrumental precision is $\sim 0.8\%$. Reproducibility determined by replicate analyses was typically better than 2%. Where replicate analyses showed a change $\leq 2\%$, the weight percent carbonate value obtained from the initial analysis is reported. When replicates varied by $>2\%$, sediment samples were reanalyzed and the final value was reported.

RESULTS

Weight percent carbonate and barite data are reported in Tables T1 and T2 and are shown in Figures F1 and F2, respectively. The CaCO_3 content of the sedimentary sections at all sites is generally high (>85 wt%) (Fig. F1). The range of carbonate content agrees with the range of shipboard carbonate analyses of E/O boundary sediment samples from Hole 1210A (90–96 wt%) (Shipboard Scientific Party, 2002). Through the sampled intervals at all sites there is a transition to a more carbonate-rich lithology that is, with few exceptions, consistent with trends in reflectance data (Fig. F1). Because a decrease in carbonate content is a feature of E/O boundary sections recovered from varied deep-sea environments, based on the observed changes in CaCO_3 , it appears that we have sampled through the Eocene–Oligocene transition at all sites.

Barite for Holes 1209A and 1210B is shown in Figure F2. A distinct maximum in barite is observed in each of these sections. The maximum barite in Hole 1209A is 0.3 wt%, whereas it is 0.1 wt% in Hole 1210B. However, these differences may be a consequence of a change in the relative quantities of carbonate and barite. To determine whether the downhole trends and/or the difference in the downhole trends are driven by differences in carbonate content, barite and carbonate content of the same sediment samples are directly compared (Fig. F3). The barite data do not correspond directly with carbonate, suggesting that high barite content is not solely a result of changes in the dilution factor by carbonate. Rather, the absence of a significant negative correlation between barite and carbonate may indicate that, at times, high organic carbon export flux is associated with high accumulation of carbonate in the sediment, possibly as a result of elevated biogenic calcite deposition.

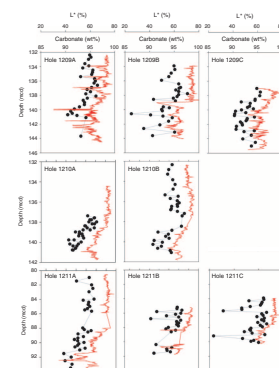
SUMMARY

Barite accumulation in marine sediments is a good proxy for export production. Fluctuations in the barite accumulation rate across the E/O boundary can therefore shed light on changes in export production as a trigger/response to changes in oceanic circulation and climate. The carbonate content of pelagic sediments is influenced by several processes, including total production in the overlying water column, changes in the relative contribution of coccolithophores to total productivity, depth, and alkalinity of bottom waters. Reliable records of export production using marine barite may be able to constrain the influence of productivity on calcium carbonate accumulation trends and lead to more reliable interpretations of the history of the CCD and the causes for dissolution/preservation events.

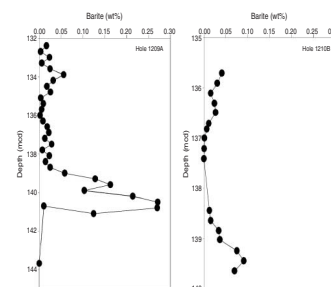
T1. Carbonate content of E/O boundary sediment, Sites 1209–1212, p. 14.

T2. Barite data across the E/O boundary, Sites 1209 and 1210, p. 16.

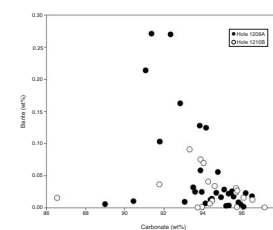
F1. Downcore trends in CaCO_3 content, Sites 1209–1211, p. 11.



F2. Barite data across the E/O boundary, Sites 1209 and 1210, p. 12.



F3. Relative barite and carbonate content, p. 13.



ACKNOWLEDGMENTS

The authors would like to thank the Leg 198 Science Party and the *JOIDES Resolution* staff and crew for the ultimate success of the cruise. This research used samples and/or data provided by the Ocean Drilling Program (ODP). ODP is sponsored by the U.S. National Science Foundation (NSF) and participating countries under management of Joint Oceanographic Institutions (JOI), Inc. This work was funded by a JOI-U.S. Science Support Program (USSSP) Grant to A. Paytan and K.B. Averyt. Funding for M. Calhoun and L. Schmalz was provided by a Stanford Undergraduate Research Fellowship (VPUE grant to AP). Many thanks to B. Jones for assistance with SEM screening of barite samples; D. Mucciarone and K. Kryc for help with carbonate analyses; J. Street, K. Faul, and A. Ivy for aid with barite separations; J. Ingle, L. Clarke, D. Thomas, and J. Zachos for helpful comments; and the staff at the ODP Gulf Coast Repository for help with sampling.

REFERENCES

- Bains, S., Norris, R.D., Corfield, R.M., and Faul, K.L., 2000. Termination of global warmth at the Palaeocene–Eocene boundary through productivity feedback. *Nature*, 407:171–174.
- Berger, W.H., Smetacek, V.S., and Wefer, G., 1989. Ocean productivity and paleoproductivity: an overview. In Berger, W.H., Smetacek, V.S., and Wefer, G. (Eds.), *Productivity of the Oceans: Present and Past*: New York (Wiley and Sons), 1–34.
- Bishop, J.K.B., 1988. The barite-opal-organic carbon association in oceanic particulate matter. *Nature*, 332:341–343.
- Bonn, W.J., Gingele, F.X., Grobe, H., Mackensen, A., and Fütterer, D.K., 1998. Palaeoproductivity at the Antarctic continental margin: opal and barium records for the last 400 ka. *Palaeogeogr., Palaeoclimat., Palaeoecol.*, 139:195–211.
- Broecker, W.S., and Peng, T.-H., 1982. *Tracers in the Sea*: Palisades, NY (Eldigio Press).
- Calvert, S.E., 1966. Accumulation of diatomaceous silica in sediments of the Gulf of California. *Geol. Soc. Am. Bull.*, 77:569–596.
- DeConto, R.M., and Pollard, D., 2003. Rapid Cenozoic glaciation of Antarctica induced by declining atmospheric CO₂. *Nature*, 421:245–249.
- Dehairs, F., Baeyens, W., and Goeyens, L., 1992. Accumulation of suspended barite at mesopelagic depths and export production in the Southern Ocean. *Science*, 258:1332–1335.
- Deuser, W.G., Ross, E.H., and Anderson, R.F., 1981. Seasonality in the supply of sediments to the deep Sargasso Sea and implications for the rapid transfer of matter to the deep ocean. *Deep-Sea Res., Part A*, 28:495–505.
- Diester-Haass, L., 1995. Middle Eocene to early Oligocene paleoceanography of the Antarctic Ocean (Maud Rise, ODP Leg 113, Site 689): change from a low to a high productivity ocean. *Palaeogeogr., Palaeoclimatol., Palaeoecol.*, 113:311–334.
- Diester-Haass, L., 1996. Late Eocene–Oligocene paleoceanography in the southern Indian Ocean (ODP Site 744). *Mar. Geol.*, 96:99–119.
- Diester-Haass, L., and Zahn, R., 1996. Eocene–Oligocene transition in the Southern Ocean: history of water mass circulation and biological productivity. *Geology*, 24:163–166.
- Dymond, J., Suess, E., and Lyle, M., 1992. Barium in deep-sea sediment: a geochemical proxy for paleoproductivity. *Paleoceanography*, 7:163–181.
- Eagle, M., Paytan, A., Arrigo, K., Van Dijken, G., and Murray, R., 2003. A comparison between excess barium and barite as indicators of carbon export. *Paleoceanography*, 18:1021.
- Ehrmann, W.U., and Mackensen, A., 1992. Sedimentological evidence for the formation of an East Antarctic ice sheet in Eocene/Oligocene time. *Palaeogeogr., Palaeoclimatol., Palaeoecol.*, 93:85–112.
- Exon, N.F., Kennett, J.P., Malone, M.J., and Leg 189 Shipboard Party, 2002. Drilling reveals climatic consequences of Tasmanian Gateway opening. *Eos, Trans. Am. Geophys. Union*, 83(23):253, 258–259.
- Faul, K., Anderson, L., and Delaney, M., 2003. Late Cretaceous and early Paleogene nutrient and paleoproductivity records from Blake Nose, western North Atlantic Ocean. *Paleoceanography*, 3:1042.
- Francois, R., Honjo, S., Manganini, S.J., and Ravizza, G.E., 1995. Biogenic barium fluxes to the deep sea: implications for paleoproductivity reconstruction. *Global Biogeochem. Cycles*, 9:289–303.
- Ganeshram, R., Francois, R., Commeau, J., and Brown-Leger, S., 2003. An experimental investigation of barite formation in seawater. *Geochim. Cosmochim. Acta*, 67:2599–2605.
- Gingele, F., and Dahmke, A., 1994. Discrete barite particle and barium as tracers of paleoproductivity in South Atlantic sediments. *Paleoceanography*, 9:151–168.

- Goldberg, E., Somayajulu, B., Gallway, J., Kaplan, I., and Faure, G., 1969. Differences between barites of marine and continental origins. *Geochim. Cosmochim. Acta*, 33:287–289.
- Goni, M.A., Ruttenger, K.C., and Eglinton, T.I., 1998. A reassessment of the sources and importance of land-derived organic matter in surface sediments from the Gulf of Mexico. *Geochim. Cosmochim. Acta*, 62:3055–3075.
- Herguera, J.C., 2000. Last glacial paleoproductivity patterns in the eastern equatorial Pacific: benthic foraminifera records. *Mar. Micropaleontol.*, 40:259–275.
- Herguera, J.C., and Berger, W.H., 1991. Paleoproductivity from benthic foraminifera abundance: glacial to postglacial change in the west-equatorial Pacific. *Geology*, 19:1173–1176.
- Kennett, J.P., 1977. Cenozoic evolution of Antarctic glaciation, the circum-Antarctic Ocean, and their impact on global paleoceanography. *J. Geophys. Res.*, 82:3843–3860.
- Kennett, J.P., and Shackleton, N.J., 1976. Oxygen isotopic evidence for the development of the psychrosphere 38 Myr ago. *Nature*, 260:513–515.
- Klump, J., Hebbeln, D., and Wefer, G., 2001. High concentrations of biogenic barium in Pacific sediments after Termination I—a signal of changes in productivity and deep water chemistry. *Mar. Geol.*, 177:1–11.
- Lear, C.H., Elderfield, H., and Wilson, P.A., 2000. Cenozoic deep-sea temperatures and global ice volumes from Mg/Ca in benthic foraminiferal calcite. *Science*, 287:269–272.
- Loubere, P., 1999. A multiproxy reconstruction of biological productivity and oceanography in the eastern equatorial Pacific for the past 30,000 years. *Mar. Micropaleontol.*, 37:173–198.
- McManus, J., Dymond, J., Dunbar, R., and Collier, R., 2002. Particulate barium fluxes in the Ross Sea. *Mar. Geol.*, 184:1–15.
- Miller, K., Fairbanks, R., and Mountain, G., 1987. Tertiary oxygen isotope synthesis, sea level history, and continental margin erosion. *Paleoceanography*, 2:1–19.
- Miller, K.G., Wright, J.D., and Fairbanks, R.G., 1991. Unlocking the Ice House: Oligocene–Miocene oxygen isotopes, eustasy, and margin erosion. *J. Geophys. Res.*, 96:6829–6848.
- Müller, P.J., and Suess, E., 1979. Productivity, sedimentation rate, and sedimentary organic matter in the oceans, I. Organic carbon preservation. *Deep-Sea Res., Part A*, 26:1347–1362.
- Nilsen, E., Anderson, L., and Delaney, M., 2003. Paleoproductivity, nutrient burial, climate change and the carbon cycle in the western equatorial Atlantic across the Eocene/Oligocene boundary. *Paleoceanography*, 18:1057.
- Nurnberg, C.C., Bohrmann, G., and Schlüter, M., 1997. Barium accumulation in the Atlantic sector of the Southern Ocean: results from 190,000-year record. *Paleoceanography*, 12:594–603.
- Pagani, M., Freeman, K., and Arthur, M., 1999. Late Miocene atmospheric CO₂ concentration and expansion of C₄ grasses. *Science*, 285:876–879.
- Paytan, A., and Kastner, M., 1996. Benthic Ba fluxes in the central Equatorial Pacific, implications for the oceanic Ba cycle. *Earth Planet. Sci. Lett.*, 142:439–450.
- Paytan, A., Kastner, M., and Chavez, F., 1996. Glacial to interglacial fluctuations in productivity in the equatorial Pacific as indicated by marine barite. *Science*, 274:1355–1357.
- Pearson, P.N., and Palmer, M.R., 2000. Atmospheric carbon dioxide concentrations over the past 60 million years. *Nature*, 406:695–699.
- Pfeifer, K., Kasten, S., Hensen, C., and Schulz, H., 2001. Reconstruction of primary productivity from the barium contents in surface sediments of the South Atlantic Ocean. *Mar. Geol.*, 177:13–24.
- Ravizza, G., and Peucker-Ehrenbrink, B., 2003. The marine ¹⁸⁷Os/¹⁸⁸Os record of the Eocene–Oligocene transition: the interplay of weathering and glaciation. *Earth Planet. Sci. Lett.*, 210:151–165.

- Raymo, M.E., and Ruddiman, W.F., 1992. Tectonic forcing of late Cenozoic climate. *Nature*, 359:117–122.
- Retallack, G.J., 2001. A 300 million-year record of atmospheric carbon dioxide from fossil plant cuticles. *Nature*, 411:287–290.
- Revelle, R., 1955. On the history of the oceans. *J. Mar. Res.*, 14:446–461.
- Ruhlemann, C., Frank, M., Hale, W., Mangini, A., Multitza, S., Muller, P.J., and Wefer, G., 1996. Late Quaternary productivity changes in the western equatorial Atlantic: evidence from ^{230}Th -normalized carbonate and organic carbon accumulation rates. *Mar. Geol.*, 135:127–152.
- Sarnthein, M., Winn, K., Duplessy, J.-C., and Fontugne, M.R., 1988. Global variations of surface ocean productivity in low and mid latitudes: influence on CO_2 reservoirs of the deep ocean and atmosphere during the last 21,000 years. *Paleoceanography*, 3:361–399.
- Shipboard Scientific Party, 2002. Leg 198 Preliminary Report. *ODP Prelim. Rpt.*, 98 [Online]. Available from World Wide Web: <http://www-odp.tamu.edu/publications/prelim/198_prel/198PREL.PDF>.
- Tappan, H., 1968. Primary production, isotopes, extinctions and the atmosphere. *Palaeogeogr., Palaeoclimatol., Palaeoecol.*, 4:185–210.
- Wright, J.D., and Miller, K.G., 1993. Southern Ocean influences on late Eocene to Miocene deep-water circulation. In Kennett, J.P., and Warnke, D.A. (Eds.), *The Antarctic Paleoenvironment: A Perspective on Global Change*. Antarct. Res. Ser., 60:1–25.
- Zachos, J., Pagani, M., Sloan, L., Thomas, E., and Billups, K., 2001. Trends, rhythms, and aberrations in global climate 65 Ma to present. *Science*, 292:686–693.
- Zachos, J.C., Quinn, T.M., and Salamy, K., 1996. High resolution (10^4 yr) deep-sea foraminiferal stable isotope records of the Eocene–Oligocene climate transition. *Paleoceanography*, 11:251–266.
- Zachos, J.C., Stott, L.D., and Lohmann, K.C., 1994. Evolution of early Cenozoic marine temperatures. *Paleoceanography*, 9:353–387.

Figure F1. Downcore trends in calcium carbonate content at Sites 1209–1211. Carbonate content (circles) with shipboard reflectance (L^*) data (red line) are shown and plotted against the meters composite depth (mcd) scale. Replicate analyses of sediment samples show that data were reproducible within 2% of the original analyses. Initial data are reported here. Where duplicate analyses varied by more than 2%, a third analysis was performed. Reflectance is a proxy of carbonate content, so it is expected that carbonate content based on coulometric analyses will vary similarly with reflectance trends.

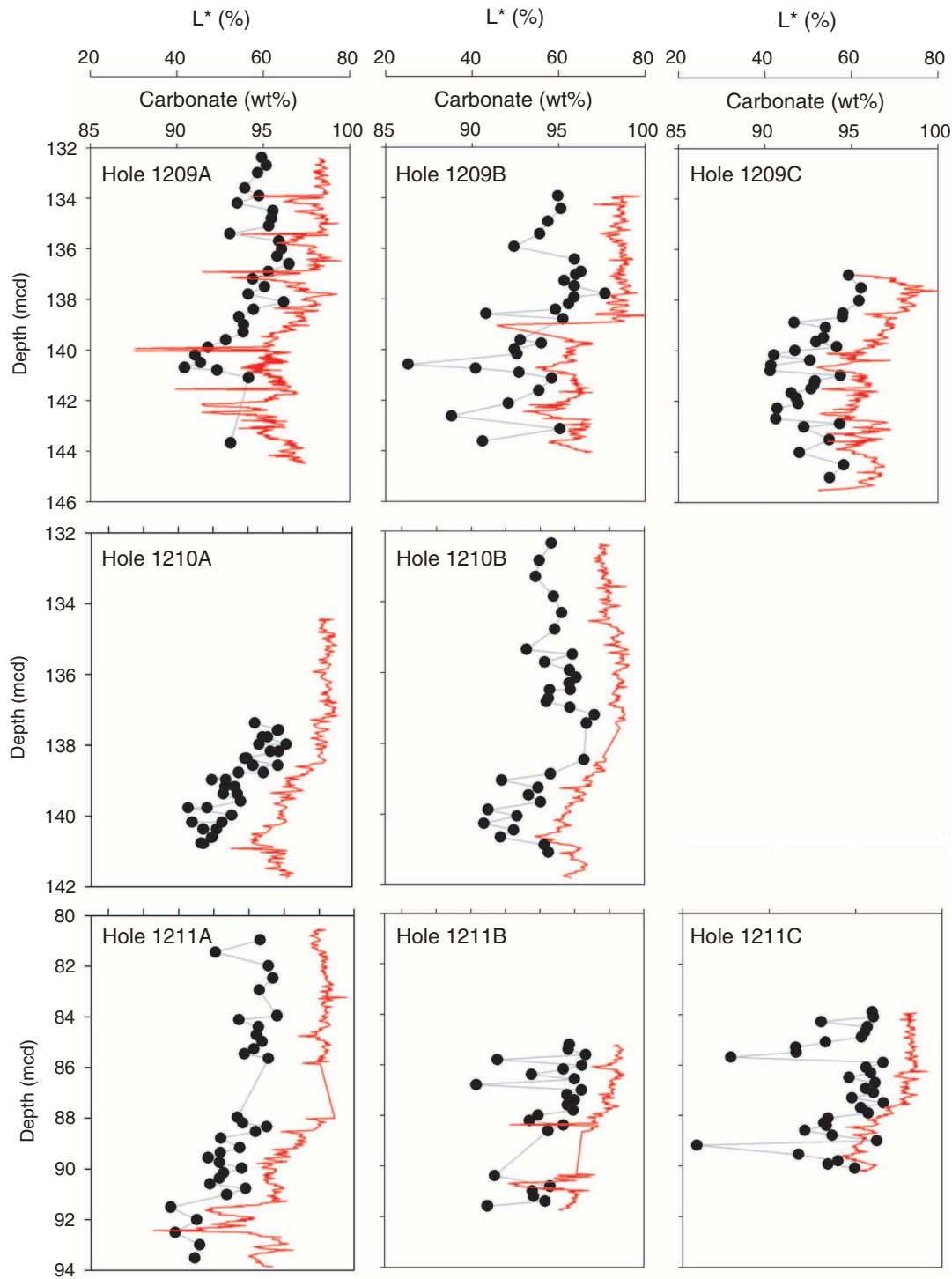


Figure F2. Barite at Sites 1209 and 1210 across the E/O boundary. Barite content was determined relative to the total quantity of sediment from which barite was extracted (see text).

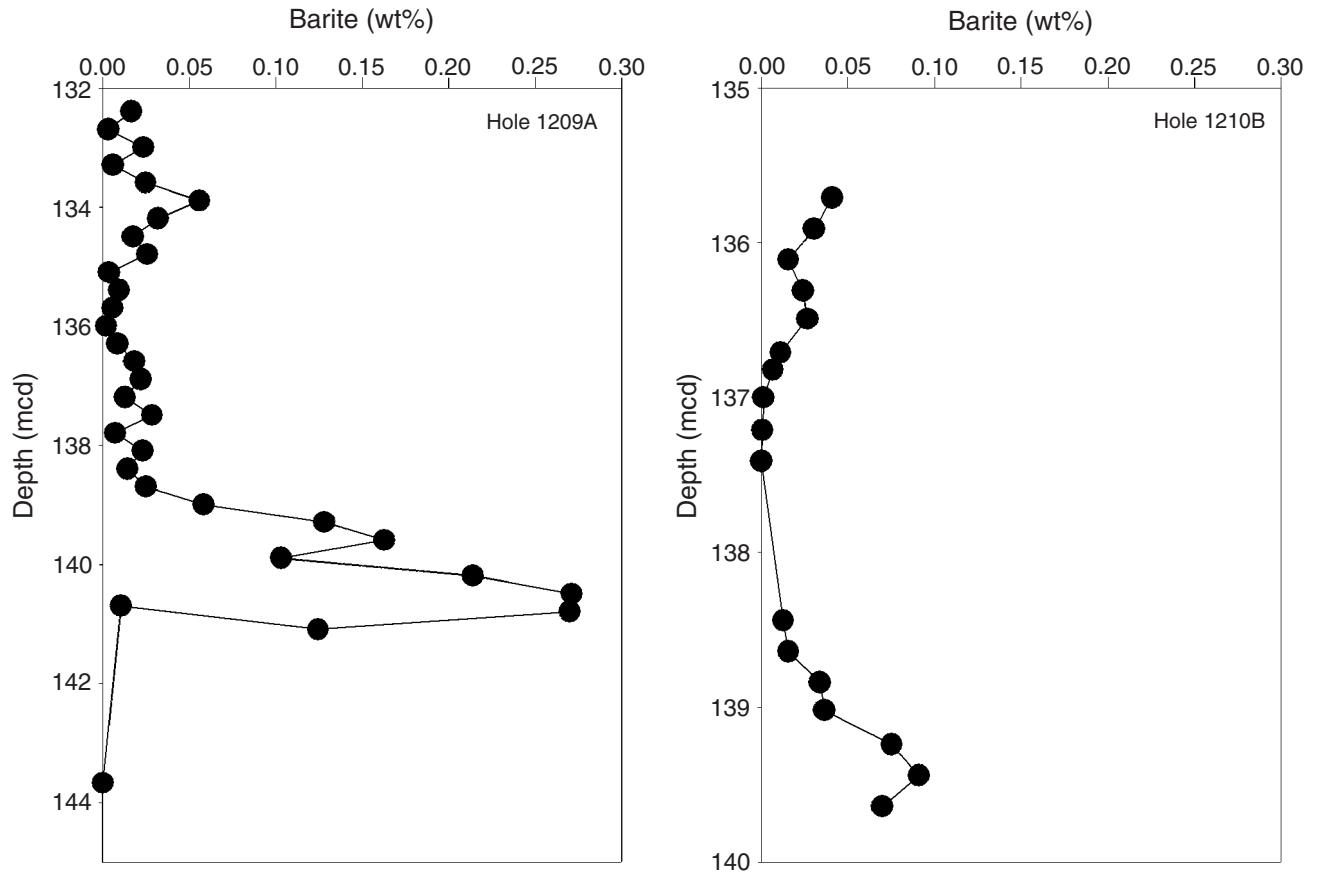


Figure F3. Relative barite and carbonate content of discrete sediment samples. Comparison of the barite and carbonate content of the same sediment sample shows that changes in the relative quantity of carbonate are not the only factors controlling downcore trends in barite.

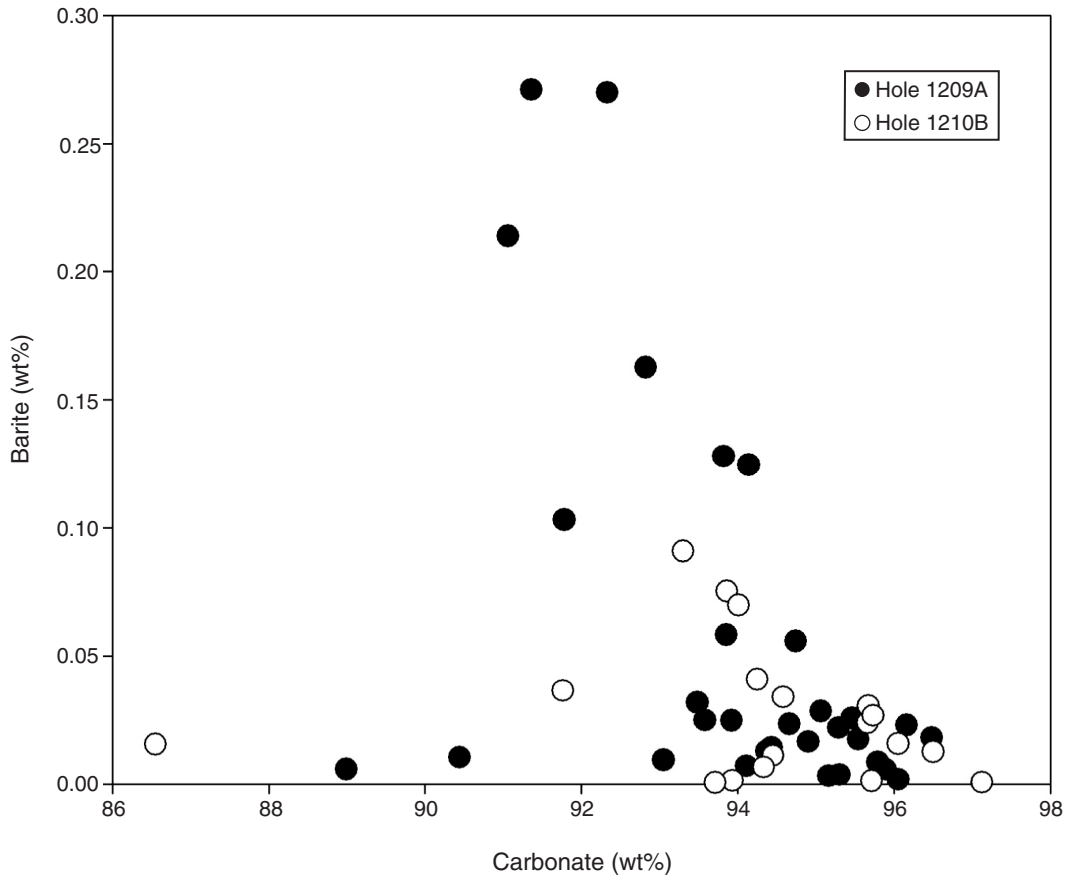


Table T1. Carbonate content of Eocene/Oligocene boundary sediment sections at ODP Sites 1209–1212. (See table notes. Continued on next page.)

Core, section, interval (cm)	Depth (mbsf)	Depth (mcd)	Carbonate (wt%)	Core, section, interval (cm)	Depth (mbsf)	Depth (mcd)	Carbonate (wt%)	Core, section, interval (cm)	Depth (mbsf)	Depth (mcd)	Carbonate (wt%)
198-1209A-				4H-2, 5–7	128.1	138.5	94.5	13H-4, 98–100	119.2	133.3	93.7
14H-1, 0–6	122.2	132.4	94.9	4H-2, 21–23	128.2	138.7	94.5	13H-5, 4–6	119.7	133.9	94.8
14H-1, 30–36	122.5	132.7	95.2	4H-2, 42–44	128.4	138.9	91.7	13H-5, 50–52	120.2	134.3	95.2
14H-1, 60–66	122.8	133.0	94.7	4H-2, 62–64	128.6	139.1	93.5	13H-5, 96–98	120.7	134.8	94.8
14H-1, 90–96	123.1	133.3	89.0	4H-2, 83–85	128.8	139.3	87.3	13H-6, 4–6	121.2	135.4	93.2
14H-1, 120–126	123.4	133.6	93.9	4H-2, 103–105	129.0	139.5	93.4	13H-6, 17–19	121.4	135.5	95.9
14H-2, 0–6	123.7	133.9	94.7	4H-2, 118–120	129.2	139.6	93.0	13H-6, 39–41	121.6	135.7	94.3
14H-2, 30–36	124.0	134.2	93.5	4H-2, 139–141	129.4	139.8	94.2	13H-6, 62–64	121.8	135.9	95.7
14H-2, 60–66	124.3	134.5	95.5	4H-3, 4–6	129.5	140.0	91.7	13H-6, 82–84	122.0	136.1	96.1
14H-2, 90–96	124.6	134.8	95.5	4H-3, 21–23	129.7	140.2	90.5	13H-6, 99–101	122.2	136.3	95.7
14H-2, 120–126	124.9	135.1	95.3	4H-3, 42–44	129.9	140.4	92.6	13H-6, 117–119	122.4	136.5	95.7
14H-3, 0–6	125.2	135.4	93.1	4H-3, 62–64	130.1	140.6	90.3	13H-6, 117–119	122.4	136.5	94.5
14H-3, 30–36	125.5	135.7	95.9	4H-3, 83–85	130.3	140.8	90.3	13H-6, 142–144	122.6	136.7	94.5
14H-3, 60–66	125.8	136.0	96.1	4H-3, 103–105	130.5	141.0	94.4	13H-7, 1–4	122.7	136.8	94.3
14H-3, 90–96	126.1	136.3	95.8	4H-3, 123–125	130.7	141.2	92.9	13H-7, 17–19	122.9	137.0	95.7
14H-3, 120–126	126.4	136.6	96.5	4H-3, 139–141	130.9	141.3	92.8	13H-7, 38–40	123.1	137.2	97.1
14H-4, 0–6	126.7	136.9	95.3	4H-4, 5–7	131.1	141.5	92.7	13H-7, 62–64	123.3	137.4	96.7
14H-4, 30–36	127.0	137.2	94.4	4H-4, 21–23	131.2	141.7	91.5	14H-1, 12–14	123.3	138.5	96.5
14H-4, 60–66	127.3	137.5	95.1	4H-4, 42–44	131.4	141.9	91.8	14H-1, 32–34	123.5	138.7	86.6
14H-4, 90–96	127.6	137.8	94.1	4H-4, 63–65	131.6	142.1	91.9	14H-1, 52–54	123.7	138.9	94.6
14H-4, 120–126	127.9	138.1	96.2	4H-4, 82–84	131.8	142.3	90.7	14H-1, 70–72	123.9	139.0	91.8
14H-5, 0–6	128.2	138.4	94.4	4H-4, 103–105	132.0	142.5	81.4	14H-1, 91–93	124.1	139.3	93.9
14H-5, 30–36	128.5	138.7	93.6	4H-4, 123–125	132.2	142.7	90.6	14H-1, 112–114	124.3	139.5	93.3
14H-5, 60–66	128.8	139.0	93.9	4H-4, 143–145	132.4	142.9	94.3	14H-1, 131–133	124.5	139.7	94.0
14H-5, 90–96	129.1	139.3	93.8	4H-5, 6–8	132.6	143.0	92.2	14H-2, 3–5	124.7	139.9	91.0
14H-5, 120–126	129.4	139.6	92.8	4H-5, 56–58	133.1	143.5	93.7	14H-2, 21–23	124.9	140.1	92.6
14H-6, 0–6	129.7	139.9	91.8	4H-5, 106–108	133.6	144.0	92.0	14H-2, 42–44	125.1	140.3	90.7
14H-6, 30–36	130.0	140.2	91.1	4H-6, 106–108	133.6	144.0	82.4	14H-2, 61–63	125.3	140.5	92.4
14H-6, 60–66	130.3	140.5	91.4	4H-6, 6–8	134.1	144.5	94.6	14H-2, 81–83	125.5	140.7	91.7
14H-6, 90–96	130.6	140.8	92.3	4H-6, 56–58	134.6	145.0	93.7	14H-2, 102–104	125.7	140.9	94.2
14H-6, 120–126	130.9	141.1	94.1	198-1210A-				14H-2, 123–125	125.9	141.1	94.5
15H-1, 68–70	132.4	140.7	90.4	14H-3, 0–3	122.9	137.4	94.4	198-1211A-			
15H-3, 66–67	135.4	143.7	93.1	14H-3, 20–22	123.1	137.6	95.8	9H-4, 4–7	73.8	81.0	94.6
198-1209B-				14H-3, 21–22	123.1	137.6	95.7	9H-4, 53–55	74.3	81.5	92.1
14H-4, 6–8	123.7	133.9	95.0	14H-3, 40–42	123.3	137.8	94.9	9H-4, 106–108	74.9	82.0	95.1
14H-4, 56–58	124.2	134.4	95.1	14H-3, 40–41	123.3	137.8	95.1	9H-5, 4–5	75.3	82.5	95.4
14H-4, 106–108	124.7	134.9	94.4	14H-3, 60–61	123.5	138.0	96.2	9H-5, 52–54	75.8	83.0	94.6
14H-5, 6–8	125.2	135.4	93.9	14H-3, 60–62	123.5	138.0	94.6	9H-6, 3–5	76.8	84.0	95.6
14H-5, 56–58	125.7	135.9	92.4	14H-3, 80–81	123.7	138.2	95.3	9H-6, 18–20	77.0	84.1	93.4
14H-5, 106–108	126.2	136.4	95.9	14H-3, 80–82	123.7	138.2	95.8	9H-6, 47–49	77.3	84.4	94.5
14H-6, 5–7	126.7	136.9	96.3	14H-3, 100–102	123.9	138.4	93.8	9H-6, 78–80	77.6	84.7	94.4
14H-6, 16–18	126.8	137.0	96.0	14H-3, 100–101	123.9	138.4	93.9	9H-6, 105–107	77.9	85.0	94.8
14H-6, 41–43	127.0	137.3	95.3	14H-3, 120–121	124.1	138.6	95.7	9H-6, 133–135	78.1	85.3	94.3
14H-6, 62–64	127.2	137.5	95.9	14H-3, 120–122	124.1	138.6	94.3	9H-7, 3–5	78.3	85.5	93.7
14H-6, 92–94	127.5	137.8	97.7	14H-3, 140–142	124.3	138.8	94.9	9H-7, 21–23	78.5	85.6	95.1
14H-6, 106–108	127.7	137.9	95.9	14H-3, 140–141	124.3	138.8	93.5	10H-1, 2–4	78.8	88.0	93.4
14H-6, 132–134	127.9	138.2	95.6	14H-4, 10–11	124.5	139.0	91.9	10H-1, 24–26	79.0	88.2	93.6
14H-7, 4–6	128.1	138.4	94.8	14H-4, 10–12	124.5	139.0	92.7	10H-1, 38–40	79.2	88.3	95.0
14H-7, 22–24	128.3	138.6	90.8	14H-4, 30–31	124.7	139.2	93.3	10H-1, 58–60	79.4	88.5	94.4
14H-7, 42–44	128.5	138.8	95.2	14H-4, 30–32	124.7	139.2	92.7	10H-1, 84–86	79.6	88.8	92.4
15H-1, 5–7	128.7	139.6	92.8	14H-4, 50–51	124.9	139.4	93.4	10H-1, 121–124	80.0	89.2	93.5
15H-1, 18–20	128.8	139.7	94.0	14H-4, 50–52	124.9	139.4	92.6	10H-1, 140–144	80.2	89.4	92.4
15H-1, 42–44	129.0	140.0	92.5	14H-4, 71–73	125.1	139.6	93.6	10H-2, 11–13	80.4	89.6	91.7
15H-1, 61–63	129.2	140.2	92.6	14H-4, 90–92	125.3	139.8	91.7	10H-2, 29–31	80.6	89.7	92.3
15H-1, 102–104	129.6	140.6	86.3	14H-4, 90–91	125.3	139.8	90.6	10H-2, 52–54	80.8	90.0	93.6
15H-1, 118–120	129.8	140.7	90.2	14H-4, 110–112	125.5	140.0	93.1	10H-2, 71–73	81.0	90.2	92.6
15H-1, 134–136	129.9	140.9	92.7	14H-4, 130–132	125.7	140.2	92.5	10H-2, 92–94	81.2	90.4	92.3
15H-2, 6–8	130.2	141.1	94.6	14H-4, 130–131	125.7	140.2	90.8	10H-2, 114–116	81.4	90.6	91.8
15H-2, 56–58	130.7	141.6	93.9	14H-5, 0–2	125.9	140.4	91.4	10H-2, 132–134	81.6	90.8	93.8
15H-2, 106–108	131.2	142.1	92.1	14H-5, 0–1	125.9	140.4	92.2	10H-3, 6–8	81.9	91.0	92.7
15H-3, 6–8	131.7	142.6	88.8	14H-5, 22–24	126.1	140.6	92.0	10H-3, 56–58	82.4	91.5	89.5
15H-3, 56–58	132.2	143.1	95.1	14H-5, 23–24	126.1	140.6	91.9	10H-3, 106–108	82.9	92.0	91.0
15H-3, 106–108	132.7	143.6	90.6	14H-5, 40–42	126.3	140.8	91.3	10H-4, 6–8	83.4	92.5	89.8
198-1209C-				14H-5, 41–42	126.3	140.8	91.5	10H-4, 54–56	83.8	93.0	91.2
4H-1, 6–8	126.6	137.0	94.8	198-1210B-				10H-4, 107–109	84.4	93.5	90.9
4H-1, 56–58	127.1	137.5	95.6	13H-4, 4–6	118.2	132.4	94.6	198-1211B-			
4H-1, 106–108	127.6	138.0	95.4	13H-4, 52–54	118.7	132.8	93.9	9H-5, 3–5	78.3	85.2	95.7

Table T1 (continued).

Core, section, interval (cm)	Depth (mbsf)	Depth (mcd)	Carbonate (wt%)
9H-5, 21-23	78.5	85.4	95.6
9H-5, 43-45	78.7	85.6	96.6
9H-5, 62-64	78.9	85.8	91.5
9H-5, 85-87	79.2	86.0	96.4
9H-5, 101-103	79.3	86.2	95.3
9H-5, 122-124	79.5	86.4	93.5
9H-5, 140-143	79.7	86.6	96.0
9H-6, 12-14	79.9	86.8	90.3
9H-6, 33-35	80.1	87.0	96.4
9H-6, 52-54	80.3	87.2	95.6
9H-6, 72-74	80.5	87.4	96.0
9H-6, 92-94	80.7	87.6	95.6
9H-6, 113-115	80.9	87.8	95.9
9H-6, 132-134	81.1	88.0	93.9
9H-7, 4-6	81.3	88.2	93.4
9H-7, 22-24	81.5	88.4	95.3
9H-7, 44-46	81.7	88.6	94.5
10H-1, 11-13	82.2	90.4	91.4
10H-1, 53-55	82.6	90.8	94.6
10H-1, 72-74	82.8	91.0	93.6
10H-1, 93-95	83.0	91.2	93.6
10H-1, 112-114	83.2	91.4	94.3
10H-1, 131-133	83.4	91.6	90.9
198-1211C-			
9H-3, 3-5	76.8	83.9	96.0
9H-3, 22-24	77.0	84.1	96.0
9H-3, 42-44	77.2	84.3	93.0
9H-3, 62-64	77.4	84.5	95.7
9H-3, 82-84	77.6	84.7	95.5
9H-3, 102-104	77.8	84.9	95.3
9H-3, 122-124	78.0	85.1	93.3
9H-3, 142-144	78.2	85.3	91.5
9H-4, 12-14	78.4	85.5	91.6
9H-4, 32-34	78.6	85.7	87.8
9H-4, 53-54	78.8	85.9	96.6
9H-4, 72-74	79.0	86.1	95.6
9H-4, 93-95	79.2	86.3	95.9
9H-4, 112-114	79.4	86.5	94.6
9H-4, 133-135	79.6	86.7	96.1
9H-5, 5-7	79.9	86.9	95.6
9H-5, 22-24	80.0	87.1	96.0
9H-5, 42-44	80.2	87.3	94.8
9H-5, 62-64	80.4	87.5	96.6
9H-5, 82-84	80.6	87.7	95.3
9H-5, 102-104	80.8	87.9	95.7
9H-5, 122-124	81.0	88.1	93.4
9H-5, 142-144	81.2	88.3	93.2
9H-6, 2-4	81.3	88.4	93.3
9H-6, 21-23	81.5	88.6	92.1
9H-6, 41-43	81.7	88.8	93.6
9H-6, 62-64	81.9	89.0	96.2
9H-6, 80-82	82.1	89.2	85.8
9H-6, 116-118	82.5	89.5	91.7
9H-6, 141-143	82.7	89.8	94.0
9H-7, 4-6	82.8	89.9	93.4
9H-7, 21-23	83.0	90.1	95.0

Notes: Replicate analyses of sediment samples show that data were reproducible within 2% of the original analyses. Initial data are reported here. Where duplicate analyses varied by >2%, a third analysis was performed.

Table T2. Barite data across the Eocene/Oligocene boundary, Sites 1209 and 1210.

Core, section, interval (cm)	Depth (mbsf)	Depth (mcd)	Barite (wt%)
198-1209B-			
14H-1, 0-6	122.2	132.4	0.02
14H-1, 30-36	122.5	132.7	0.00
14H-1, 60-66	122.8	133.0	0.02
14H-1, 90-96	123.1	133.3	0.01
14H-1, 120-126	123.4	133.6	0.02
14H-2, 0-6	123.7	133.9	0.06
14H-2, 30-36	124.0	134.2	0.03
14H-2, 60-66	124.3	134.5	0.02
14H-2, 90-96	124.6	134.8	0.03
14H-2, 120-126	124.9	135.1	0.00
14H-3, 0-6	125.2	135.4	0.01
14H-3, 30-36	125.5	135.7	0.01
14H-3, 60-66	125.8	136.0	0.00
14H-3, 90-96	126.1	136.3	0.01
14H-3, 120-126	126.4	136.6	0.02
14H-4, 0-6	126.7	136.9	0.02
14H-4, 30-36	127.0	137.2	0.01
14H-4, 60-66	127.3	137.5	0.03
14H-4, 90-96	127.6	137.8	0.01
14H-4, 120-126	127.9	138.1	0.02
14H-5, 0-6	128.2	138.4	0.01
14H-5, 30-36	128.5	138.7	0.02
14H-5, 60-66	128.8	139.0	0.06
14H-5, 90-96	129.1	139.3	0.13
14H-5, 120-126	129.4	139.6	0.16
14H-6, 0-6	129.7	139.9	0.10
14H-6, 30-36	130.0	140.2	0.21
14H-6, 60-66	130.3	140.5	0.27
15H-1, 68-70	132.4	140.7	0.01
14H-6, 90-96	130.6	140.8	0.27
14H-6, 120-126	130.9	141.1	0.12
198-1210B-			
13H-6, 40-42	121.6	135.7	0.04
13H-6, 60-62	121.8	135.9	0.03
13H-6, 80-82	122.0	136.1	0.02
13H-6, 100-102	122.2	136.3	0.02
13H-6, 118-120	122.4	136.5	0.03
13H-6, 140-142	122.6	136.7	0.01
13H-7, 1-4	122.7	136.8	0.01
13H-7, 19-21	122.9	137.0	0.00
13H-7, 40-42	123.1	137.2	0.00
14H-1, 10-13	123.3	138.4	0.01
14H-1, 30-32	123.5	138.6	0.02
14H-1, 50-52	123.7	138.8	0.03
14H-1, 68-70	123.9	139.0	0.04
14H-1, 90-92	124.1	139.2	0.08
14H-1, 110-112	124.3	139.4	0.09
14H-1, 130-132	124.5	139.6	0.07